Estimating CO2 Response in a Mixed Broadleaf Forest using the Dynamic Assimilation Technique

HuiTing Hu
Beijing Forestry University
Wei Jiang
Beijing Forestry University
Xiuhua Fan
bjfanxh@bjfu.edu.cn

Beijing Forestry University

Research Article

Keywords: Dynamic assimilation technique, CO2 response, Mixed broadleaf-Korean pine forest, photosynthetic physiological traits

Posted Date: July 15th, 2024

DOI: https://doi.org/10.21203/rs.3.rs-4552226/v1

Additional Declarations: No competing interests reported.

Version of Record: A version of this preprint was published at BMC Plant Biology on January 21st, 2025.
See the published version at https://doi.org/10.1186/s12870-024-05912-w.

Estimating CO_2 Response in a Mixed Broadleaf Forest using the Dynamic Assimilation Technique

Author

Huiting Hu, Wei Jiang, Xiuhua Fan

Corresponding author

Xiuhua Fan, bjfanxh@bjfu.edu.cn

Institution

College of Science, Beijing Forestry University, Beijing, China

Abstract

Background: Estimating the CO_2 response of forest trees is of great significance in plant photosynthesis research . CO_2 response measurement is traditionally employed under steady state conditions. With the development of open-path gas exchange systems, the Dynamic Assimilation Technique (DAT), allows measurement under non-steady state conditions. This greatly improves the efficiency and data density of CO_2 response measurement. However, the effects of different models in fitting the DAT data have not been extensively verified. **Results:** This research was conducted for three common broadleaf tree species (*Ulmus macrocarpa*, *Fraxinus mandshurica*, and *Tilia amurensis*) in North Eastern China. Among the three species, Fraxinus mandshurica is the most adapted to high CO_2 concentration conditions. Four models were compared, the rectangular hyperbola (RH) model, the Michaelis-Menten (MM) model, the modified rectangular hyperbola (MRH) model and a non-rectangular hyperbola (NRH) model. **Conclusions:** Considering the model parsimony and parameter accuracy , the NRH model emerged as the best choice (R^2=0.9966, RMSE=0.1862, AIC=-199.86). This study provides a reference for the further application of DAT in the field of photosynthesis.

Keywords: Dynamic assimilation technique, CO_2 response, Mixed broadleaf-Korean pine forest, photosynthetic physiological traits

1 Background

Photosynthesis is an elementary and important physiological process of plant growth, providing the material foundation and energy source for life on Earth. The CO_2 concentration of the atmosphere is one of the key factors influencing plant photosynthesis. Measuring the CO_2 response of plant photosynthesis allows for the determination of important photosynthetic parameters such as CO_2 compensation point (Γ), CO_2 saturation point, carboxylation rate (V_c), and electron transport rate (J) [1]. These parameters are crucial for studying plant photosynthesis and predicting global carbon cycle fluxes. Traditional measurements of the CO_2 response (A-C_i) curve use steady-state measurements, requiring a series of predetermined CO_2 concentrations. The photosynthetic rate won't be recorded until the measured leaves stabilize at each CO_2 concentration for 1 to 3 minutes. Obtaining a steady-state A-C_i curve with more than ten data points typically takes over 30 minutes [1]. This measurement protocol is time-consuming as it requires a significant amount of time to obtain the photosynthetic rate at several specified concentrations. Additionally, plants are susceptible to changes in their physiological state due to environmental influences during the measurement[1]. Prolonged measurement duration may result in changes in enzyme activation state, chloroplast movement, or stomatal aperture[2]. There is also a risk of overfitting when fitting multiple photosynthetic parameters using a small number of data points based on steady-state measurements[3].

To improve the efficiency of obtaining CO_2 response data, Stinziano(2017) proposed a rapid A-C_i measurement technique called Rapid A-C_i Response (RACiR). But this technique requires not only pre-measurement calibration of the empty chamber to reduce errors caused by increasing CO_2 mole fractions,

but also subtracting the empty chamber values during data processing. It is a non-steady-state technique that requires empirical corrections [4, 5]. Validation studies have indicated that RACiR may lead to underestimation of parameters such as Γ and dark respiration (R_d)[6, 7] .

Dynamic Assimilation Technique (DAT) further optimizes the non-steady-state A-C_i measurement method based on RACiR [8]. With high temporal resolution, DAT can accurately calculate plant CO_2 assimilation values by using known incoming and outgoing CO_2 mole fractions, as well as well-estimated derivatives. It has broad applicability in various types of gas exchange measurements. DAT not only allows for rapid acquisition of high-density data but also reduces the oscillations in photosynthesis under triose-phosphate utilization[9]. Many studies have explored the application of DAT in measuring other important photosynthetic parameters, such as measuring photorespiration [10] and the temperature response of photosynthesis and so on. Validation studies have consistently shown no significant differences between DAT and traditional methods, while significantly improving data density and reducing noise during measurement. DAT has been applied to in-depth researches on photosynthetic mechanisms[11, 12].

Modern commercial gas exchange measurements usually follow the open path measurement principle, where a flow of air continuously enters and flows out of the leaf chamber. In the steady-state measurements, the net photosynthesis rate is calculated based on the formula as follows[13]:

$$A = \frac{u_1 c_1 - u_2 c_2}{S} \quad (1)$$

Where A represents the net photosynthesis rate ($mol \cdot m^{-2} s^{-1}$), S is leaf area (m^2), u_1 and u_2 represents the incoming and outgoing air mass flow rates ($mol \cdot s^{-1}$), $c_1$and c_2 means the incoming and outgoing mole fraction of CO_2 in the air ($mol \cdot mol^{-1}$).

During DAT measurements, the incoming and outgoing mole fraction of CO_2 and its derivative with

high temporal resolution can be estimated well, through which the accurate value of A in the non-steady state can be calculated from[8]:

$$A = \frac{u_1 c_1 - u_2 c_2 - V_\rho \frac{dc_2}{dt}}{S} \quad (2)$$

Where the meaning of A, S, u_1 and u_2, c_1 and c_2 is the same as mentioned. V represents the cuvette volume (L), ρ is the air density ($mol^{-1} \cdot L$), $\frac{dc_2}{dt}$ is the rate of change of CO_2 mole fraction in the leaf chamber ($mol \cdot mol^{-1} s^{-1}$).

Comparing equations (1) and (2), it can be concluded that the measurement under steady state is a special situation of the governing mass balance when $\frac{dc_2}{dt}$ is zero. DAT measurement can provide researchers with more comprehensive physiological data, benefit in better understanding the mechanisms of plants responding to environmental changes. The introduction of this method greatly improves the speed of field measurements of CO_2 response. It is of great significance for the accumulation of relevant data. Its high-throughput data characteristics also enable researchers to gain a deeper understanding of the mechanisms of photosynthesis.

Photosynthesis models and theories use mathematical equations and parameters to describe the processes of carbon fixation and release in photosynthesis. This makes it possible to predict and explain changes in the CO_2 response. Existing A-C_i curve fitting models include rectangular hyperbolic model[14], Michaelis-Menten model[15], non-rectangular hyperbolic model[16], modified rectangular hyperbolic model[17] etc. As a high-density continuous measurement method, DAT measurement can effectively shorten the measurement range and improve measurement efficiency by choosing an appropriate and effective fitting model. Currently, there is no relevant comparison and validation of the fitting effects of various models under the DAT measurement. Therefore, this study compares the fitting effects of different models on various photosynthetic limitations stages and photosynthetic parameters

based on the DAT measurement of three typical broad-leaved tree species in a mixed broad-leaved-Korean pine forest.

2 Materials and Methods

2.1 Study area

The study was conducted in a 100m×100m plot of mixed broadleaf-Korean pine forest located within the Jiaohe Experimental Area Management Bureau in Jilin Province, China (127° 45′ E, 43° 57′ N). The area is part of the Zhangguangcai Mountains in the Changbai Mountain Range and experiences a temperate continental monsoon climate, with an average elevation of 459 m, an annual mean temperature of 3.5 ℃ and a mean temperature of 21.7℃ in July. The annual average precipitation is 695.9 mm, mainly concentrated in July and August. The soil in the region is classified as dark brown forest soil, with a soil layer thickness ranging from 20 to 80 cm. The vegetation in the study area belongs to the Changbai Mountain flora, with the dominant forest type being mixed broad-leaved-Korean pine forest. The main tree species include *Pinus koraiensis*, *Quercus mongolica*, *Tilia amurensis*, *Ulmus davidiana*, *Fraxinus mandshurica*, *Ulmus macrocarpa*, *Juglans mandshurica*, *Acer mono* and *Acer mandshuricum* .

2.2 Sampling method

Typical broad-leaved tree species in this area were selected as the research subjects, including *Ulmus macrocarpa* (*U.macrocarpa*), *Fraxinus mandshurica* (*F.mandshurica*) and *Tilia amurensis* (*T.amurensis*). For each species, we sampled 13 individuals with an approximate diameter at breast height of 10 cm. And for each chosen individual, we sampled 3 healthy and intact mature leaves for gas exchange measurements.

2.3 CO_2 response measurement

We conducted gas exchange measurements using the portable photosynthesis measurement system Li-6800, manufactured by LiCor Corporation. Measurements were conducted during clear weather conditions, from 8:30 AM to 11:30 AM and from 2:00 PM to 4:30 PM. In order to maintain consistency in measurements, all leaves were measured in a detached state. Secondary branches with favorable light conditions were selected from each target tree using high branch shears. Immediately after cutting, the branch tips were submerged in water to maintain internal water potential and prevent leaf dehydration. Throughout the measurement process, the branch tips were kept continuously submerged to preserve leaf condition. The environmental parameters are presented in table 1. Prior to running each experiment, the leaves were allowed to adapt to these conditions until stomatal conductance (g_s) and A reached a stable state.

Table 1 Environmental parameters settings

Internal Name	Units	Descrition	Set value
Qin	$\mu mol \cdot m^{-2}s^{-1}$	PPFD incident on the leaf	1500
Flow	$\mu mol \cdot s^{-1}$	Flow rate into chamber	500
Tleaf	℃	Leaf thermocouple	25
C2O_r	$\mu mol \cdot mol^{-1}$	Reference cell CO, concentration	400
H2O_r	%	Reference cell H,O concentration	60

2.3.1 Steady-state measurement

A single sample tree of *Tilia amurensis* was selected for the steady-state measurement study. Two healthy, intact, and mature leaves chosen from the sunlit branches of the tree were prepared for steady-state and non-steady-state measurements respectively. The goal was to compare the differences between traditional steady-state measurements and non-steady-state measurements using the DAT protocol.

The steady-state measurements were conducted at CO2 concentrations of 400, 300, 200, 100, 50, 25, 15, 10, 200, 400, 600, 800, 900, 1000 and 1200 $\mu mol \cdot mol^{-1}$, with a minimum waiting time of 90s and

a maximum waiting time of 150s for each CO_2 concentration.

2.3.2 Non-steady state DAT measurement

A total of 117 leaves (n=117) were selected from 13 sample trees of three different tree species for non-steady-state gas exchange measurements. The DAT measurement available on Li-6800 was employed to measure the CO_2 response. Prior to measurement, a range match was performed to account for changes in CO_2 concentration. Calibration of CO_2 and H_2O was conducted daily to minimize measurement errors and determine the optimal slope. The measurements were carried out using a BP program, with each leaf acclimatized in the leaf chamber until g_s and A stabilized. The starting CO_2 concentration of the curve was set at 10 μmol·mol^{-1}, with a pre-slope waiting time of 2 minutes. The final concentration was set at 1210 μmol·mol^{-1}, with a concentration increase rate (Ramp rate) of 100 μmol·mol^{-1}·min^{-1}. The total measurement time was approximately 14 minutes.

2.4 Models

In addition to the biochemical model Farquhar-von Caemmerer-Berry (FvCB) model, there are simplified empirical models used for fitting the CO_2 response process. The mainstream models include the Michaelis-Menten (MM) model, the modified rectangular hyperbola (MRH) model, the non-rectangular hyperbola (NRH) model and the rectangular hyperbola (RH) model.

2.4.1 The FvCB model

The FvCB model is widely used for simulating photosynthesis response [18]. It is a mechanistic model based on biochemical processes, describing the response of photosynthetic rate to light intensity, CO_2 concentration, and temperature. It utilizes a set of differential equations to simulate the relationship between photosynthetic rate and related variables, including excitation of photosynthetic pigments, carbon reactions, and light reactions. However, the FvCB model has many parameters .

151 **2.4.2 The Michaelis-Menten model**

152 The Michaelis-Menten (MM) model, as used by Harley[15], is expressed by the equation:

153 $$A_n = \frac{A_{nmax}C_i}{C_i+K} - R_P \quad (3)$$

154 Where A_n represents the net photosynthetic rate, C_i is the intercellular CO_2 concentration, α is the initial

155 carboxylation rate corresponding to the slope of the linear equation when CO_2 concentration $\leqslant$ 200

156 μmol·mol^{-1}, A_{nmax} is the maximum net photosynthetic rate, R_P is the rate of photorespiration, and K is the

157 Michaelis-Menten constant.

158 **2.4.3 The Modified Rectangular Hyperbola**

159 The modified rectangular hyperbola (MRH) , as used by Ye[17], is expressed by the equation:

160 $$A_n = \alpha\frac{1-bC_i}{1+cC_i}C_i - R_P \quad (4)$$

161 Where the definition of A_n, C_i, α, A_{nmax} and R_P is the same as mentioned above. b is the modification

162 coefficient of the model, and c is the ratio of α and A_{nmax} (both b and c are in units of mol·μmol-1).

163 **2.4.4 The Non-rectangular Hyperbola**

164 The non-rectangular hyperbola (NRH) , as used by Thornley[19], is expressed by the equation:

165 $$A_n = \frac{\alpha C_i+A_{nmax}-\sqrt{(\alpha C_i+A_{nmax})^2-4\theta\alpha C_i A_{nmax}}}{2\theta} - R_P \quad (5)$$

166 Where the definition of A_n, C_i, α, A_{nmax} and R_P is the same as mentioned above, and θ represents the

167 curvature of the A_n-C_i curve.

168 **2.4.5 Rectangular hyperbola model**

169 The rectangular hyperbola (RH) model, derived from Baly's formula[14], is expressed by the

170 equation:

171 $$A_n = \frac{\alpha A_{nmax}C_i}{\alpha C_i + A_{nmax}} - R_P \quad (6)$$

172 Where the definition of A_n, C_i, α, A_{nmax} and R_P is the same as mentioned above.

2.5 Data processing and analysis

The model fitting for the test data was implemented using the "plantecophys" package in R. The four empirical models were fitted using the photosynthesis calculation software developed by Ye. The C_{isat} values for RH model, NRH model and MM model were obtained using the equation $A_{max} = \alpha C_{isat} - R_P$. The accuracy of model fitting for photosynthetic parameters was assessed using mean absolute error (MAE). The performance of the models was assessed by the coefficients of determination (R^2), root mean square error (RMSE) and Akaike information criterion (AIC). The best combination with the largest R^2 value, smallest RMSE and AIC values represented the best accuracy.

To mitigate the impact of data noise on the visualization of the model curves and better reflect the overall trend of the response curves, local weighted scatterplot smoothing (Loess smoothing) was applied during curve visualization, with a smoothing span set at 0.8.

3 Result

3.1 Comparing steady-state and DAT measurements

In the experiment of two sample leaves using different measurement protocols, the steady-state measurement took a total of 25 minutes, obtaining 14 data points. The non-steady state DAT measurement took a total of 12 minutes, obtaining 336 data points. Completing the measurement in a

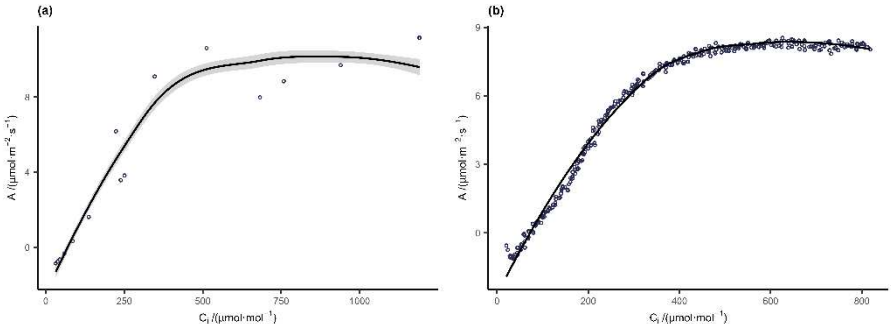

Fig. 1 Example of traditional steady-state measurement (left) and DAT measurement (right)

shorter time also reduces the possibility of data fluctuations caused by sudden environmental changes.

It became evident that DAT can obtain denser data points in a shorter amount of time (Fig. 1). High-throughput data provides a valuable resource for calculating a wide range of photosynthesis-related parameters. Due to the limitations of measurement speed, steady-state measurements are usually unable to obtain many data points to observe response fluctuations at high concentrations. A lack of data points during the triose phosphate utilization (TPU) phase prevents accurate fitting of TPU values.

In contrast, DAT measurement allows for better observation of data fluctuations during the dynamic changes in CO_2 concentration.

3.2 Fitting of photosynthetic parameters

3.2.1 Photosynthesis biochemical parameters fitting with FvCB model

Using the FvCB model, four important photosynthesis biochemical parameters were fitted,

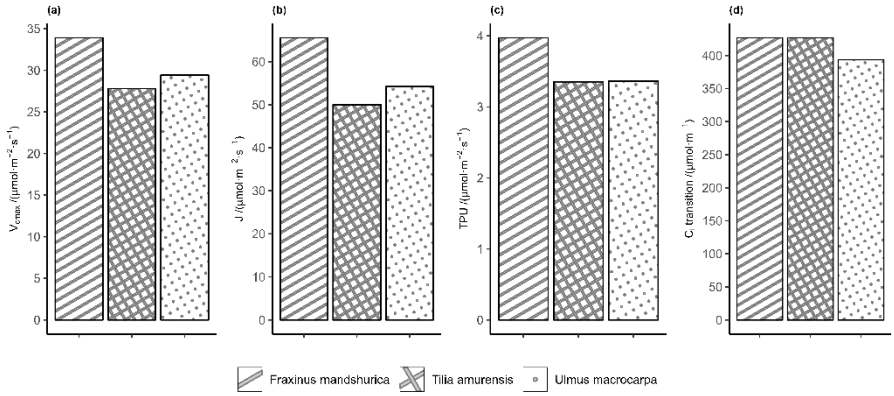

Fig. 2 Comparison of photosynthesis biochemical parameters among species. (a) The

including the maximum carboxylation rate (V_{cmax}), J , TPU, and C_i transition point ($C_{i,trans}$, the transition point where carboxylation limitations are replaced by electron transport limitations). A comparison of the model parameters for the three species is shown in Fig. 2

Among the three tree species, the V_{cmax}, J, and TPU values of the *F.mandshurica* were relatively high, indicating its higher productivity, photosynthetic efficiency, and stress resistance, allowing it to better adapt to high light intensity and high CO_2 concentration environments.

3.2.2 Photosynthesis characteristic parameter fitting using empirical models

All four models show good fitting results for Γ, with the NRH model providing the most accurate simulation. The NRH model fits well for the initial carboxylation efficiency (α), while the other models tend to overestimate this parameter to varying degrees. In terms of fitting the maximum net photosynthetic rate (A_{max}), both the M-M model and RH model significantly overestimate the results, while the MRH model and NRH model estimate values close to the actual measurements. Among them, the MRH model provides more accurate and stable simulation (Table 2).

Table 2 Comparison of models fitting photosynthesis parameters

Species	Models	α	MAE (α)	A_{max}	MAE (A_{max})	C_{isat}	MAE (C_{isat})	Γ	MAE (Γ)	R_p
U.macrocarpa	MM	-	-	21.31	12.21	887.41	304.28	71.01	1.69	3.74
	MRH	0.0414	0.0135	9.43	0.37	631.13	56.58	72.52	1.32	2.78
	NRH	0.0306	0.0027	11.78	2.69	459.10	146.30	70.87	0.96	2.14
	RH	0.0668	0.0388	21.31	12.21	417.86	212.15	71.01	1.69	3.74
	Observed	0.0279	-	9.09	-	604.85	-	71.96	-	-
F.mandshurica	MM	-	-	27.71	18.73	1085.26	471.45	103.08	3.25	6.66
	MRH	0.0514	0.0169	10.57	0.44	655.43	62.23	105.06	1.92	4.89
	NRH	0.0373	0.0029	15.11	5.42	516.90	116.87	105.20	0.89	3.92
	RH	0.0894	0.0550	27.71	18.73	453.40	185.43	103.08	3.25	6.66
	Observed	0.0344	-	10.19	-	628.62	-	105.84	-	-
T.amurensis	MM	-	-	18.62	9.83	958.06	288.37	70.46	3.29	3.34
	MRH	0.0376	0.0137	9.02	0.23	698.00	51.18	73.57	1.75	2.50
	NRH	0.0274	0.0035	11.22	2.42	487.83	209.47	73.64	0.84	1.97
	RH	0.0605	0.0366	18.62	9.83	392.82	308.60	70.46	3.29	3.34
	Observed	0.0238	-	8.78	-	696.82	-	73.28	-	-

Both the M-M model and RH model perform poorly in estimating the intercellular CO_2 saturation concentration (C_{isat}), with the estimated results significantly higher than the actual measurements. The

NRH model, on the other hand, underestimates this parameter, while the MRH model accurately fits the results with no significant difference from the observed value ($P>0.05$). Considering the RMSE of the fitted parameters, the NRH model has better estimation performance for α, while the MRH model performs better in estimating A_{max} and C_{isat}. If only the value of Γ is required, any of the four models can be used for estimation.

3.3 CO_2 response curve fitting using empirical models

The curves of each tree species were divided into three CO_2 limitation stages based on the mean values of $C_{i,trans}$ and actual C_{isat} to observe the fitting performance of different models in each limitation stage. By observing the fitted A-C_i curves, all four models fit well in the Rubisco limitation stage, but the MM model and RH model have overall lower fitting values in the RuBP limitation stage. In the final

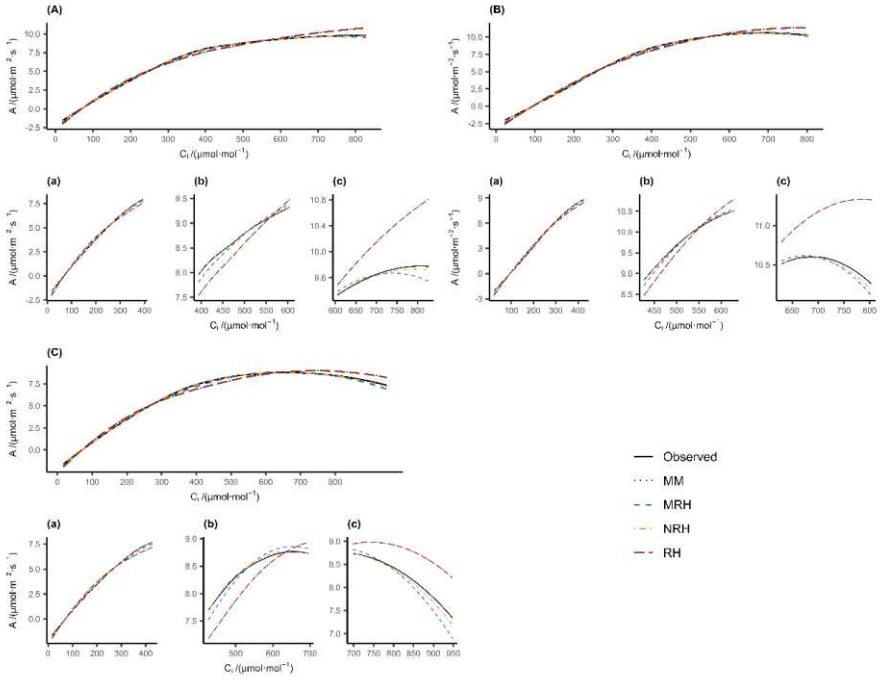

Fig. 3 Comparison of models fitting response curves. (a) Fitting results in Rubisco limited condition. (b) Fitting results in RuBP limited condition. (c) Fitting results in TPU-limited

TPU limitation stage, the MM model and RH model do not converge, resulting in overestimation of A_{max}.

227 Overall, the MRH model and NRH model show high agreement with the actual measured curves
228 throughout the process (Figure 3).

229 The residuals are presented in Fig. 4.

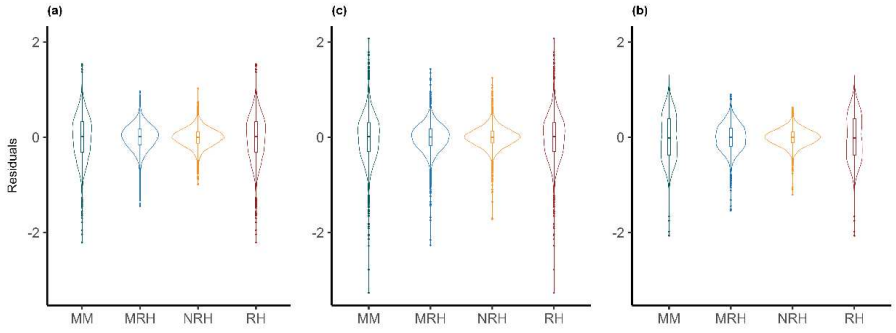

Fig. 4 Residuals of models fitting response curves. (a) The residuals of fitting models for *U.macrocarpa*. (b) The residuals of fitting models for *F. mandshurica*. (c) The residuals of fitting models for *T.amurensis*

230 Based solely on R^2, all four models show good fitting performance for the CO_2 response curves.
231 However, from the RMSE values and residual distribution plots, it can be seen that the MRH model and
232 NRH model show a better performance for the three tree species, with smaller and more concentrated
233 residuals, indicating relatively accurate predictions. On the other hand, the MM model and RH model
234 exhibit poorer performance, with large residuals, dispersed ranges, and more outliers, indicating an
235 inability to accurately fit certain parts of the entire curve. While RMSE and R^2 can measure the fitting
236 accuracy of models, they cannot effectively evaluate the complexity of the models and assess overfitting .
237 Therefore, using AIC values to assess the fitting accuracy as well as model complexity, the NRH model
238 has significantly lower AIC values compared to the other models for all tree species (Table 3).

239 Table 3 Performance of models fitting response curves

Species	Assessment	Models

		MM	MRH	NRH	RH
U.macrocarpa	R^2	0.9804	0.9931	0.9960	0.9804
	RMSE	0.4270	0.2507	0.1862	0.4271
	AIC	375.79	18.42	-189.83	375.80
F.mandshurica	RMSE	0.9860	0.9941	0.9966	0.9860
	R^2	0.4216	0.2586	0.1948	0.4216
	AIC	366.73	43.36	-158.85	366.74
T.amurensis	RMSE	0.9778	0.9927	0.9972	0.9778
	R^2	0.4643	0.2672	0.1679	0.4643
	AIC	444.55	68.61	-250.88	444.57

In the A-C_i curves of the three tree species, *F.mandshurica* exhibits lower A at low CO_2 concentrations compared to the other tree species, and it also has a higher Γ value, indicating that *F.mandshurica* requires higher CO_2 concentrations for normal photosynthesis. *F.mandshurica* also has a higher α value compared to the other species, and it's a A value increases rapidly with increasing C_i, demonstrating its adaptability and responsiveness to changes in CO_2 concentration. After the response curve stabilizes, *F.mandshurica* also has the highest A_{max}.

U.macrocarpa and *T.amurensis* have similar photosynthetic rates at low CO_2 concentrations, and their rate increases gradually, showing differences in the response curves only at $C_i > 200\mu mol \cdot mol^{-1}$. When the photosynthetic rate reaches a certain value, *U.macrocarpa* saturates at a C_i concentration of $600\mu mol \cdot mol^{-1}$, while *T.amurensis* continues to slowly increase until it saturates at nearly $700\mu mol \cdot mol^{-1}$.

Comparing the goodness of fit of the response curves for the three tree species, the simulation performance for the response curve of *F.mandshurica* is relatively poor, while the response curve of *T.amurensis* has a good fit. In terms of curve shape, the response curve of *U.macrocarpa* levels off after $C_i > 400\mu mol \cdot mol^{-1}$ and has a clear inflection point, while the curves of *F.mandshurica* and *T.amurensis*

gradually become smoother only after C_i > 500μmol·mol^{-1}. After C_i > 650μmol/mol, the photosynthetic rate of *T.amurensis* shows a significant decline, and a similar trend can be observed in *F.mandshurica* after C_i > 700μmol·mol^{-1}, although this result is not statistically significant. *U.macrocarpa* does not show a decline in A within the measured range after reaching C_i saturation.

4 Discussion

4.1 The application of DAT

The Dynamic Assimilation Technique is currently the most efficient method for plant CO_2 response curve measurement. It can complete measurement twice as fast as the traditional steady-state measurement method while data accuracy ensured[3]. The duration for a DAT measurement can even be limited in 10min according to the specific requirements by narrowing the measurement range or speeding up the ramp rate [12]. In this study, using the DAT protocol, an average of 345 data points were obtained in each measurement of CO_2 response, and each response curve took 14 minutes to complete. A high rate of observations was acquired within a short time.

In addition to significantly improving the efficiency and accuracy of conventional measurements, DAT also facilitates researches focusing on the physiological mechanisms of plant photosynthesis. Some existing studies have benefited from the efficient measurements provided by DAT. This efficient new protocol allows for more accurate experimental designs to compare the physiological changes in plant photosynthesis under different limiting conditions[20–23]. The application of DAT has also inspired the development of other dynamic assimilation methods, such as the FAsTeR method [11] and the $Laisk_{DAT}$ method [10]. These non-steady state measurement protocols offer higher measurement speed and denser data points compared to steady-state methods. In addition to ensuring plant activity during measurements, new non-steady state protocols also provided higher data densities, which contributes to the confidence

of parameter estimation and reduces the influence of noise. Moreover, DAT measurements can help reveal physiological characteristics that are difficult to observe in steady-state measurements. For example, plants require reaching the TPU limitation rapidly to induce oscillation, which can only be achieved using DAT. The rapid increase in CO_2 concentration conducted by the DAT effectively induces oscillation in the TPU limitation stage, allowing for the study of limitations on the receptor side of Photosystem I [9, 24].

It is evident that DAT method has significant advantages and broad prospects in the field of photosynthesis. Its efficiency and accuracy provide researchers with more data as well as possibilities to deepen the exploration of photosynthetic physiological mechanisms. And thus, it offers new ideas and methods for more efficient photosynthesis research.

4.2 The CO_2 response of the three tree species studied

Among three species measured, *F.mandshurica* has a higher Γ value, which means it needs a higher CO_2 concentration to achieve normal photosynthetic rates. In contrast, *U.macrocarpa* and *T.amurensis* have relatively similar Γ value. Correspondingly, *F.mandshurica* has a higher A_{max} compared to the other two tree species. This indicates that *F.mandshurica* can better adapt to high CO_2 concentrations and exhibits higher photosynthetic efficiency under such conditions.

Both *U.macrocarpa* and *F.mandshurica* have similar C_{isat} values, requiring about 600μmol·mol^{-1} to reach CO_2 saturation, while *T.amurensis* can reach saturation with a concentration around 700μmol·mol^{-1}. Among them, *U.macrocarpa* shows a rapid increase in photosynthetic rate at beginning stage, and the response curve becomes significantly flattened after reaching the $C_{i,trans}$ point. In the end, it reaches A_{max} at around 600μmol·mol^{-1}. This indicates that when Rubisco enzyme is active in U.macrocarpa , the effect of RuBP regeneration limitation becomes significant as CO_2 concentration further increases,

299 causing a significant reduction in the magnitude of the changes in the photosynthetic rate and there almost
300 no further increase. *T.amurensis* also exhibits a similar trend, with only a slight increase in the
301 photosynthetic rate under the limiting condition of the RuBP regeneration . However, compared to
302 *U.macrocarpa*, the magnitude of the changes in *T.amurensis* in the photosynthetic rate slows down
303 gradually, allowing its C_{isat} value to reach about 700μmol·mol^{-1}.

304 In contrast, the photosynthetic response curve of *F.mandshurica* continues to show a significant
305 increase after passing the $C_{i,trans}$ point until reaching saturation . This indicates that after Rubisco enzyme
306 is fully active and RuBP regeneration limits the photosynthesis rate, *F.mandshurica* exhibits a relatively
307 greater change in photosynthetic rate, suggesting a higher photosynthetic efficiency than the other two
308 species.

309 After reaching saturation, the photosynthetic rate of *U.macrocarpa* does not show significant
310 changes as C_i concentration continues to increase, while *F.mandshurica* and *T.amurensis* exhibit a
311 declining trend with increasing concentration. This may be due to the limitation of photosynthetic rate
312 by TPU at high C_i concentrations [22]. Among them, *T.amurensis* shows the most pronounced decrease.

313 Taking into account the CO_2 response characteristics and biochemical parameters of the three
314 species, it can be concluded that *F.mandshurica* is the most adapted to high CO_2 concentration conditions.
315 Previous studies have also indicated that *F.mandshurica* exhibits significantly enhanced photosynthesis
316 under high CO_2 concentration conditions [25, 26]

317 4.3 Compare fitting models

318 Although empirical models are simplified versions of the FvCB biochemical model, they have their
319 advantages. Firstly, FvCB model cannot estimate the C_{isat} and A_{max} of plants and require empirical model
320 fitting to obtain such parameters [27]. Secondly, biochemical model requires a large number of

parameters during the modeling process. It means that fitting FvCB model with a small number of data points obtained from traditional steady-state measurements may result in overparameterization[28]. Empirical models have fixed equations and fewer parameters, thus require less computation for large-scale data processing and model fitting. This advantage makes them more applicable. For individual sample measurement, empirical models are more convenient and efficient when calculation high-density data from DAT. And for meta-analyses, empirical models can better capture data patterns and be applied to models that focus on predictive performance and scale extrapolation.

Among the four models, both the MM model and RH model exhibit similar performance. The fitted A values continuously increasing with C_i without clear saturation points or stable trends. Therefore, these models perform poorly in all three model evaluation criteria and are not recommended for modeling DAT data. Nevertheless, the MRH model and NRH model show better overall performance, each with its own strengths. From the perspective of evaluating photosynthesis parameters, the NRH model performs well in fitting parameters (such as α and Γ) before reaching saturation, while the MRH model performs better in fitting parameters (such as Amax and C_{isat}) after reaching C_i saturation. In terms of simulating response curves, considering various assessment indicators, it can be concluded that the NRH model has higher fitting accuracy and better adherence to measured data. The NRH model outperforms the MRH model in terms of AIC, even though their fitting accuracy is similar. The introduction of an additional parameter in the MRH model may increase model complexity and make it more susceptible to sample size or noise data. This may lead to potential overfitting issues and limit the generality and applicability of the MRH model.

Previous studies have often considered the MRH model to perform better overall, particularly in fitting photosynthetic parameters, compared to the NRH model [29, 30]. This may because the MRH

model focuses more on the interaction effects of various factors in the photosynthetic process. But for the NRH model, it has a better ability to fit the overall distribution and trend of the measured data for a reason that it's more flexible, better able to adapt to the changes in data distribution, and good at capturing the nonlinear features of the response curve. On the other hand, in terms of parameter fitting, the NRH model and MRH model show similar performance. However, in this study, comparing the fitting performance with high-density data, it can be observed that the NRH model better matches the shape of the measured curve, which indicates that the former may reflect the physiological mechanism of CO_2 response better. Existing comparative analysis studies of high-throughput data fitting models, such as the study by Wang[31], only focused on comparing parameter fitting and did not further evaluate the accuracy of model fitting for the whole response curve.

In addition to fitting accuracy, model complexity is also an important indicator for assessing model. Considering the AIC values, this study concludes that the NRH model performs better. It can behave better when facing situations such as predicting CO_2 response for species and scaling-up models from leaf to larger scales.

5 Conclusion

Based on the data obtained from DAT measurements in a mixed broad-leaved-Korean pine forest, this study compared the fitting performance of four empirical models. Firstly, the use of DAT measurements significantly improved measurement efficiency and data density, making the changes in different limitation stages of the CO_2 response more pronounced. Secondly, results show that *F.mandshurica* is more adapted to high CO_2 concentrations compared to the other two species. Last but not least, the NRH model not only demonstrated good fitting performance but also maintained parameter parsimony. Model simplicity is an advantage when applying leaf-scale data to larger-scale models for

prediction and extrapolation. The findings of this study serve as a reference for selecting appropriate measurement protocols, selecting suitable models and providing a theoretical basis for future photosynthetic research .

Abbreviations

The following abbreviations are used in this manuscript:

Γ	CO_2 compensation point
V_c	Carboxylation rate
J	Electron transport rate
A-C_i	CO_2 response
RACiR	Rapid A-C_i Response
R_d	Dark respiration
DAT	Dynamic Assimilation Technique
A	Net photosynthesis rate
S	Leaf area
u_1 and u_2	Incoming and outgoing air mass flow rates
$c_1$and c_2	Incoming and outgoing mole fraction of CO_2 in the air
V	Cuvette volume
ρ	Air density
$\frac{dc_2}{dt}$	Rate of change of CO_2 mole fraction in the leaf chamber
g_s	Stomatal conductance
FvCB	Farquhar-von Caemmerer-Berry
MM	Michaelis-Menten
MRH	Modified rectangular hyperbola
NRH	Non-rectangular hyperbola
RH	Rectangular hyperbola

MAE	Mean absolute error
R^2	Coefficients of determination
RMSE	Root mean square error
AIC	Akaike information criterion
TPU	Triose phosphate utilization
V_{cmax}	Maximum carboxylation rate
$C_{i,trans}$	C_i transition point
α	Initial carboxylation efficiency
A_{max}	Maximum net photosynthetic rate
C_{isat}	CO_2 saturation concentration

Declarations

Ethics approval and consent to participate

Not applicable.

Consent for publication

Not applicable.

Availability of data and materials

Please contact the corresponding author for the data requests.

Competing interests

The authors declare that they have no competing interests.

Funding

This work was supported by National Key Research and Development Program of China (2022YFD2201003).

Authors' contributions

All authors contributed to the study conception and design. Material preparation, data collection and

analysis were performed by HH and WJ. The first draft of the manuscript was written by HH and all authors commented on previous versions of the manuscript. XF was responsible for reviewing and revising the script. All authors read and approved the final manuscript.

Acknowledgements

This research was funded by the Key Project of the National Key Research and Development Plan (2022YFD2201003). We thank Klaus von Gadow for correcting and improving our English language.

References

1. Long SP, Bernacchi CJ. Gas exchange measurements, what can they tell us about the underlying limitations to photosynthesis? Procedures and sources of error. J Exp Bot. 2003;54:2393–401.

2. Stinziano JR, Morgan PB, Lynch DJ, Saathoff AJ, McDermitt DK, Hanson DT. The rapid A–Ci response: photosynthesis in the phenomic era. Plant Cell Environ. 2017;40:1256–62.

3. Tejera-Nieves M, Seong DY, Reist L, Walker BJ. The Dynamic Assimilation Technique measures photosynthetic CO_2 response curves with similar fidelity as steady-state approaches in half the time. J Exp Bot. 2024;:erae057.

4. Lawrence EH, Stinziano JR, Hanson DT. Using the rapid A-Ci response (RACiR) in the Li-Cor 6400 to measure developmental gradients of photosynthetic capacity in poplar. Plant Cell Environ. 2019;42:740–50.

5. Stinziano JR, McDermitt DK, Lynch DJ, Saathoff AJ, Morgan PB, Hanson DT. The rapid A/C_i response: a guide to best practices. New Phytologist. 2019;221:625–7.

6. Coursolle C, Otis Prud'homme G, Lamothe M, Isabel N. Measuring Rapid A–Ci Curves in Boreal

404 Conifers: Black Spruce and Balsam Fir. Front Plant Sci. 2019;10.

405 7. Taylor SH, Long SP. Phenotyping photosynthesis on the limit – a critical examination of RACiR. The
406 New Phytologist. 2019;221:621–4.

407 8. Saathoff AJ, Welles J. Gas exchange measurements in the unsteady state. Plant Cell Environ.
408 2021;44:3509–23.

409 9. McClain AM, Sharkey TD. Rapid CO_2 changes cause oscillations in photosynthesis that implicate PSI
410 acceptor-side limitations. J Exp Bot. 2023;74:3163–73.

411 10. Schmiege SC, Sharkey TD, Walker B, Hammer J, Way DA. Laisk measurements in the nonsteady
412 state: Tests in plants exposed to warming and variable CO2 concentrations. Plant Physiology.
413 2023;193:1045–57.

414 11. Garen JC, Michaletz ST. Fast Assimilation-Temperature Response: a FAsTeR method for measuring
415 the temperature dependence of leaf-level photosynthesis. New Phytologist. 2024;241:1361–72.

416 12. Haque MI, Shapira O, Attia Z, Cohen Y, Charuvi D, Azoulay-Shemer T. Induction of stomatal
417 opening following a night-chilling event alleviates physiological damage in mango trees. Plant
418 Physiology and Biochemistry. 2024;206:108221.

419 13. Busch FA, Ainsworth EA, Amtmann A, Cavanagh AP, Driever SM, Ferguson JN, et al. A guide to
420 photosynthetic gas exchange measurements: Fundamental principles, best practice and potential pitfalls.
421 Plant Cell Environ. 2023. https://doi.org/10.1111/pce.14815.

14. Baly ECC. The kinetics of photosynthesis. Proceedings of the Royal Society of London Series B: Biological Sciences. 1935;117:218–39.

15. Harley PC, Thomas RB, Reynolds JF, Strain BR. Modelling photosynthesis of cotton grown in elevated CO_2. Plant Cell Environ. 1992;15:271–82.

16. Duursma RA. Plantecophys - An R Package for Analysing and Modelling Leaf Gas Exchange Data. PLoS One. 2015;10:e0143346.

17. Ye ZP. A new model for relationship between irradiance and the rate of photosynthesis in Oryza sativa. Photosynt. 2007;45:637–40.

18. Farquhar GD, von Caemmerer S, Berry JA. A biochemical model of photosynthetic CO_2 assimilation in leaves of C3 species. Planta. 1980;149:78–90.

19. Thornley JHM. Mathematical models in plant physiology. Academic Press (Inc.) London, Ltd.; 1976.

20. Arce Cubas L, Rodrigues Gabriel Sales C, Vath RL, Bernardo EL, Burnett AC, Kromdijk J. Lessons from relatives: C4 photosynthesis enhances CO_2 assimilation during the low-light phase of fluctuations. Plant Physiol. 2023;193:1073–90.

21. Gao Y, Stein M, Oshana L, Zhao W, Matsubara S, Stich B. Exploring natural genetic variation in photosynthesis-related traits of barley in the field. J Exp Bot. 2024;:erae198.

22. Gregory LM, McClain AM, Kramer DM, Pardo JD, Smith KE, Tessmer OL, et al. The triose phosphate utilization limitation of photosynthetic rate: Out of global models but important for leaf

models. Plant Cell Environ. 2021;44:3223–6.

23. Zhang C, Li Y, Yu Z, Wang G, Liu X, Liu J, et al. Co-elevation of atmospheric [CO_2] and temperature alters photosynthetic capacity and instantaneous water use efficiency in rice cultivars in a cold-temperate region. Front Plant Sci. 2022;13.

24. McClain AM, Sharkey TD. Triose phosphate utilization stress during photosynthesis addressed with dynamic assimilation measurements. 2022;:2022.11.27.518113.

25. Gao-Ming J, Chun-Mei QU. Photosynthetic Response of Six Woody Species to Elevated $COCO_2$ in Quercus liaotungensis Forest in the Beijing Mountainous Areas. Chinese Journal of Plant Ecology. 2000;24:204.

26. Zhou Y, Han S, Zhang J, Zou C, Wang C, Chen Y. Photosynthetic characteristics of three tree species seedlings in Changbai Mountain under different CO_2 concentrations. Ying Yong Sheng Tai Xue Bao. 2002;13:41–4.

27. Ye Z. A review on modeling of responses of photosynthesis to light and CO_2. Journal of Plant Ecology (Chinese Version). 2010;34:727–40.

28. Gu L, Pallardy SG, Tu K, Law BE, Wullschleger SD. Reliable estimation of biochemical parameters from C3 leaf photosynthesis–intercellular carbon dioxide response curves. Plant Cell Environ. 2010;33:1852–74.

29. Ma X, Wu C, Liu Q, Huang X. Photosynthetic CO_2 response characteristics in canopy of Larix principis-rupprechtii Mayr. tree and practicability of three Models. 2023;:2023.06.04.543630.

30. Yang S, Bao Y, Ye J, Wu S, Zhang M, Xu M, et al. Comparison of photosynthetic-CO_2 response process and models of Leymus chinensis under differing nitrogen addition and mowing conditions. Acta Prataculturae Sinica. 2023;32:160.

31. Wang X, Kang M, Wang S, Cao W, Zhu Y, Liu B. Comparison of rapid A-Ci response (RACiR) curve fitted by different photosynthetic carbon assimilation CO_2 response models in rice. Journal of Nanjing Agricultural University. 2022;45:1099–106.